4.3.2 Liquidizing Behaviors of the Powder during Heating to Semi-Solid State

The hot-consolidated Al-Si-Cu-Mg powder preforms were then reheated to a semi-solid state, at which a fraction of liquid exists appropriate for thixocasting. The adequate temperature for thixocasting was determined by a DTA test and an isothermal heat treatment test, experimental results were described as follows.

A. Phase transformation in semi-solid state

Differential Thermal Analysis (DTA) was used to reveal the semi-solid temperature range of the powder used. Three groups of the used powders - fine (<45μm), medium (45~120μm) and coarse (120~300μm), have DTA curves with almost the same features. This indicates that the three groups of powders almost have the same temperature range of semi-solid state, even though the smaller powders have finer microstructures.

Figure 4.16 plots a typical DTA curve of the powder, showing that the range of temperatures over which solidification occurs is from about 750°C to 500°C. Upon heating, two endothermic peaks appear at on-set temperatures of 523°C and 565°C. Three exothermic peaks exhibited during cooling, at on-set temperatures at 750°C, 565°C and 500°C. The onset temperature of 523°C in Fig. 4.16 is close to the ternary eutectic point of α-Al, $CuAl_2$ and Si [81, 82].

Table 4.4 lists the possible reactions of the Al-SiCuMgMn alloy during solidification [81-84]. Based on Table 4.4, we suggest that the ternary eutectic zone exhibited between α-Al grains boundaries must be first melted at above 523°C. Since the Cu content is only 2.45 wt% in this alloy, the amount of the liquid generated at this moment should be small. Nevertheless, this small amount of liquid could provide the fluidity of the powder preforms required for thixocasting; because that the powder preforms were successfully consolidated at about such temperature.

On further heating up to 565°C, the binary phases of α-Al and Si would begin to melt via the reactions 3, 4 and 5 listed in Table 4.4. This reaction will quickly deplete the α-Al solid particles in the semi-solid powder preforms. As a result, when the temperature is above 560°C, primary Si particles are completely surrounded by liquid

phase, which will result in dramatic grain growth of primary Si particles. This result of quick grain growth and the more fundamental aspects of this mechanism will be detailed in Section 4.3.3. Briefly, when the powder was heated to semi-solid state, the final temperature of the powder preforms should be controlled between 523°C ~560°C to obtain fine primary Si particles.

When the temperature reached 577°C, α-Al should melt completely via reaction 2 listed in Table 4.4, and then remain the solid phase of primary Si particles. On further heating to 750°C, the Si particles began to dissolve in the melt, as described by reaction 1 in Table 4.4.

Figure 4.16 also includes a small exothermic peak at 500°C, during cooling. However, no corresponding endothermic peak appears at 500°C during heating. This is because of the slow solidification of the powder during cooling stage in DTA testing, causing the reactions occurred, liquid → Al+ Al_2Cu+ Al_2CuMg+ Mg_2Si [81] or liquid →Al + Al_2Cu + $Al_5Mg_8Cu_2Si_6$ + Si [84]. However, the missing DTA peak at 500°C during heating may be due to the super-saturation of Mg in rapidly solidified powders.

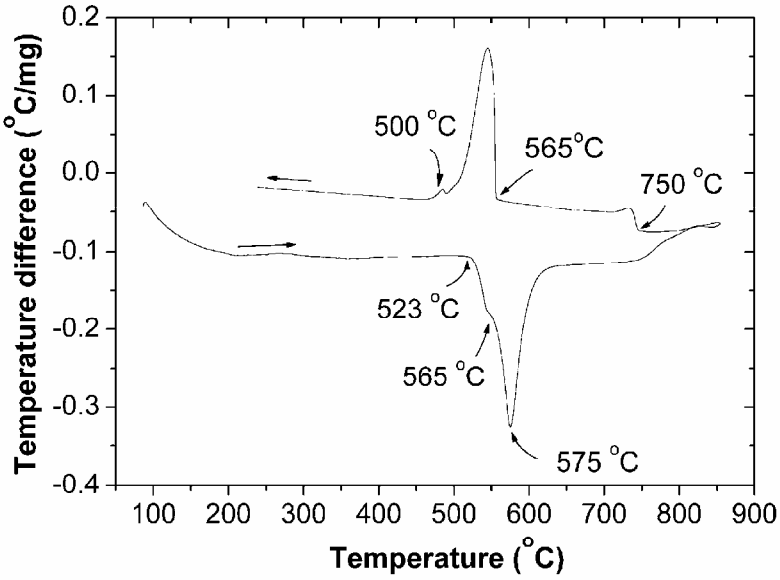

Figure 4.16 Differential thermal analyses (DTA) scan of the hypereutectic Al-25Si-2.5Cu-1Mg powder.

The powder was heated up to 800°C at rate of 10°C /min followed by cooling at rate of 10 °C /min.

Table 4.4 Possible reactions during solidification of the Al-25Si2Cu1Mg alloy

No.	Reactions	Composition			Temperature
		%Cu	%Mg	%Si	(°C)
1	Liq. →Liq. +Primary Si*	--	--	25	750
2	Liq.→Al + Si [84]	--	--	12.6	577
3	Liq.→Al + Si + Mg_2Si [84]	--	5	13	555
4	Liq.→Al + Si + Al_2Cu [82,84]	26-31	--	5-6.5	525
5	Liq.→Al + Al_2Cu + $Al_5Mg_8Cu_2Si_6$+ Si [84]				512
6	Liq.→Al + Al_2Cu + $Al_5Mg_8Cu_2Si_6$ + Si [84]	28	2.2	6	507
7	Liq. → Al+ Al_2Cu+ Al_2CuMg+ Mg_2Si [81]				500

*Estimated from binary Al-Si phase diagram [83].

B. Calculating liquid fraction from Al-Si-Cu ternary phase diagram

In semi-solid metal forming, the formability of a metal depends strongly on its thixotropic characteristics, including liquid content and microstructure. Besides the major constituents of 25wt%Si and 2.5wt%Cu, the powders used here also contain other minor elements such as 1.0 wt% Mg, 0.47wt% Mn and 0.16 wt%Fe (Table 4.1). Since the solubility of Mg in α-Al is as high as 17.1% at 450°C, the 1.0 wt% Mg could be totally dissolved in α-Al grains in as-atomized powders. Thus the 1.0 wt% Mg would not affect the liquid fraction of the powders heated from solid state into a semi-solid state. The proportions of other minor elements of Mn and Fe in the powder were too small to influence the liquid content. Consequently, a ternary Al-Si-Cu phase diagram [35], Fig. 4.17, was used here to determine the liquid content and describe the microstructural evolution of the powders in the semi-solid state.

Figure 4.17 is depicted as that proposed by P.J. Ward [35,37]. Hatched zone shows three phases region, i.e. α-Al, Si and liquid. The compositions of the powder used are about 25wt% Si and 2.5wt% Cu, which is shown at point P in this phase diagram. Dashed line A-P-B shows how equilibrium liquid contents are found using the level rule.

In a binary Al-Si alloy, solid α-Al, Si grains and liquid melt can not coexist, since

the α-Al melts completely at a eutectic temperature of 577°C. By adding some Cu to the hypereutectic Al-Si alloy, P.J. Ward [35] found that solid α-Al could be stabilized to coexist with Si grains and liquid melt, as revealed in Fig. 4.17. However, α-Al was stabilized only in the early stage of melting to a semi-solid. In this work, stabilization occurred between 530°C and 565°C, as revealed in Fig. 4.16. On further heating of the powders above 565°C, binary eutectic phases of α-Al and Si in the powders began to melt, α-Al + Si →Liquid (Table 4.4). This reaction quickly depletes the solid α-Al phase in the thixo-forming microstructured slurry, and finally solid Si grains remain suspended in the liquid melt. On further heating to 750°C, the primary Si grains dissolve completely in the melt.

Figure 4.17 presents an isothermal section of an Al-Si-Cu ternary phase diagram at 560°C [36]. Point "E" is the ternary eutectic point of α-Al, $CuAl_2$ and Si, and is the lowest point of the liquidus surface in the phase diagram. At point "E", aluminum alloy contains 26.7 wt% Cu and 5.2 wt% Si and melts at 525°C [13,15]. In Fig. 4.16, an endothermic peak occurred with onset temperature at 530°C. Since this onset temperature is close to this ternary eutectic point, we suggest that the formation of the melt starts with the ternary eutectic phases of α-Al, $CuAl_2$ and Si when the powder is heated to 530°C.

Point "B" in Fig. 4.17 is the point of intersection between the isothermal planes at 560°C and the eutectic valley. Point "P" represents the compositions of the powder used. Point "A" is the point of intersection of the line extended from point "B" through "P" with the Al/Si side of the three-phase region. Using the lever rule, the liquid fraction at 560°C can be approximated by AP/AB, at around 15wt%. This small amount of liquid may provide the fluidity required to deform the powders during powder-thixocasting.

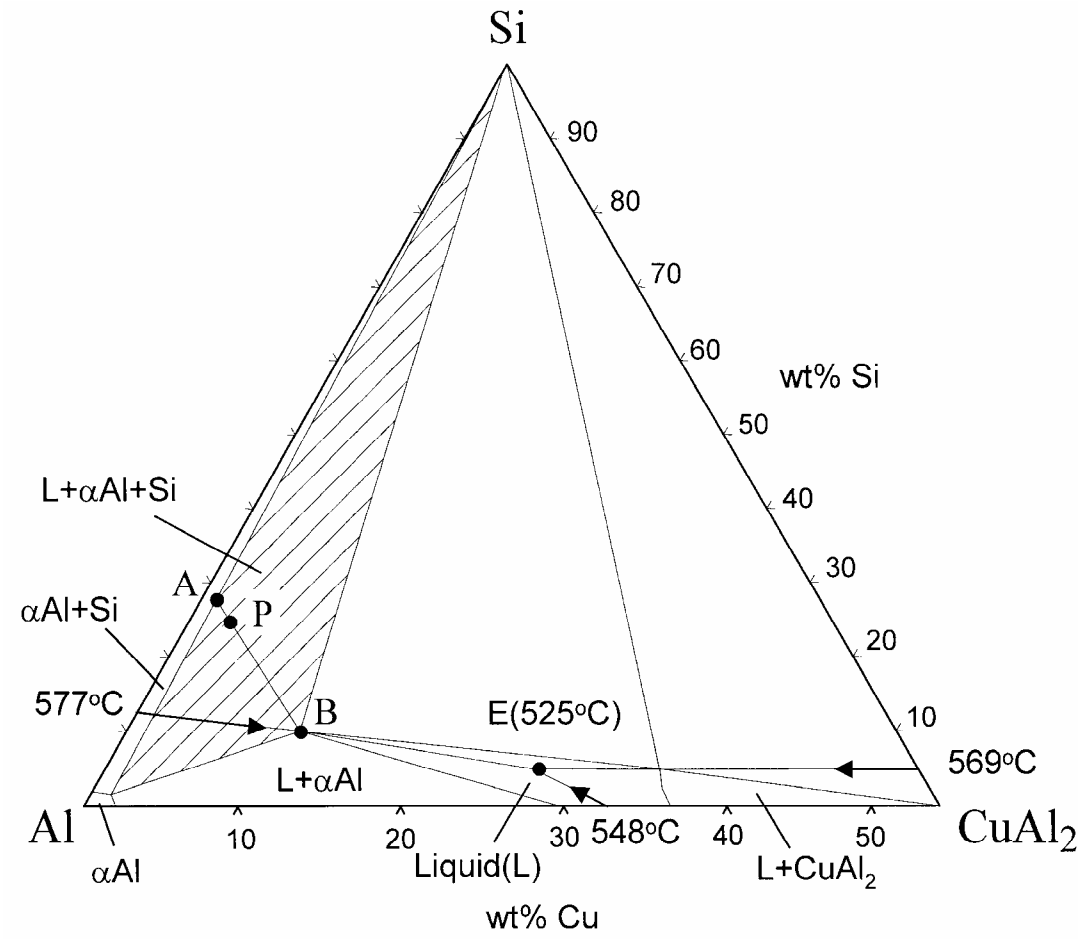

Fig.4.17 The Al-Si-Cu isothermal phase diagram at 560°C [36]

4.3.3 Kinetics of Si Grain Growth in Semi-solid State

Hypereutectic Al-Si alloys with fine Si particles are desirable for engineers. However, the semi-solid processing in which the powders are heated to a temperature between solidus and liquidus may cause the grain growth of the Si particles. Therefore, the Si grain growth kinetic at semi-solid temperatures should be concerned. Isothermal heat treatment tests were performed to elucidate the grain growth of primary Si particles during semi-solid processing of the Al-Si alloy. Results are detailed as follows.

A. Microstructural observations

Figure 4.18 shows an optical micrograph of the as-atomized hypereutectic Al-25Si-2.5Cu-1Mg-0.5Mn powder. Figures 4.19 (a)-(c) present optical micrographs of

the powders isothermally heat-treated at 500°C, 550°C and 600°C for 1 hour, respectively. Comparing Figs. 4.18 and 4.19 shows that Si grains did not clearly become coarser after they were isothermally heat-treated at 500°C and 550°C; but they did apparently become coarser after isothermal heat-treatment at 600°C for 1 hour.

It is noted in Fig.4.18 that there are black “network” in the Al-grains of the as-atomized powder. However, this network is not visible in the heat-treated powders (Fig.4.19). The micro-constituents of the black “network” (Fig.4.18) would contain the eutectic phases of α-Al and Si, which generally exhibit in the chill-cast hypereutectic Al-Si alloy, along with other phases such as Mg_2Si, Al_2Cu, $Al_{15}(Mn,Fe)_3Si_2$, $Al_5Mg_8Cu_2Si_6$ etc [81-84]. After heat treating at 500°C or 600°C, some of these phases dissolved into α-Al matrix according to the solubility of the element in α-Al. The phases that did not dissolve completely such as eutectic Si and Al_2Cu would grow up during heat-treating. This coarsening would yield several small particles distributed around the primary Si as shown in Figure 4.19.

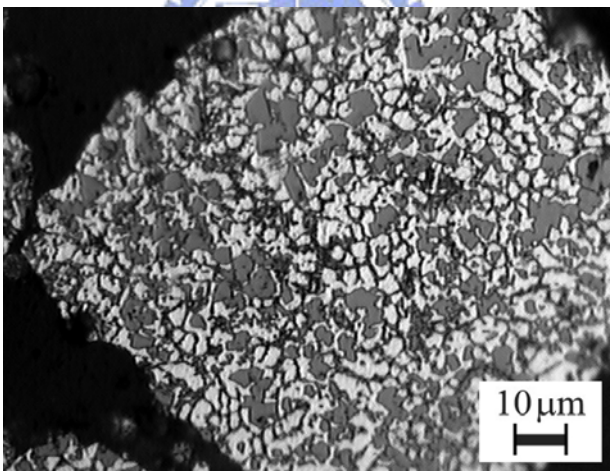

Figure 4.18 Optical microstructures of the as-atomized Al-25Si-2.5Cu-1Mg-0.5Mn powders

(a)

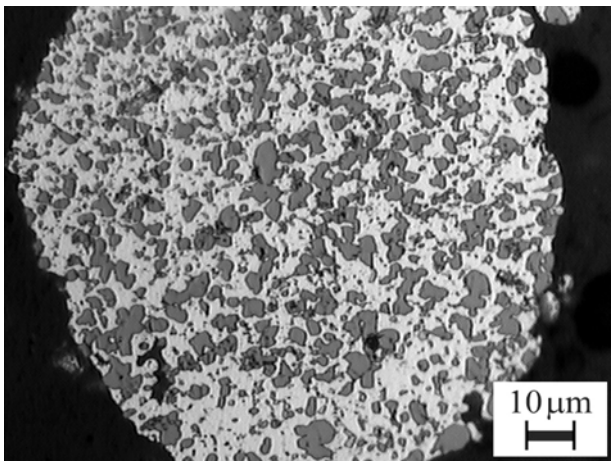

(b)

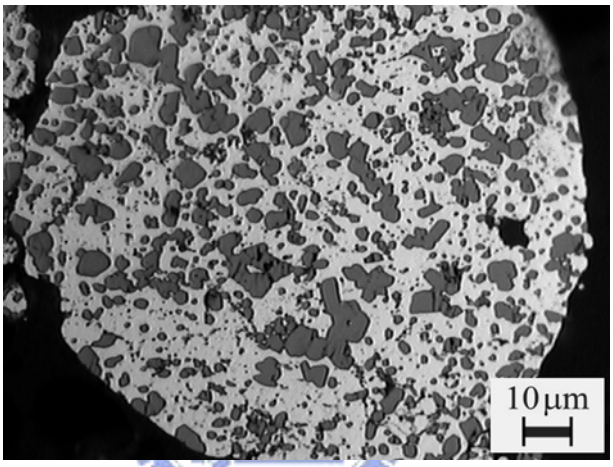

(c)

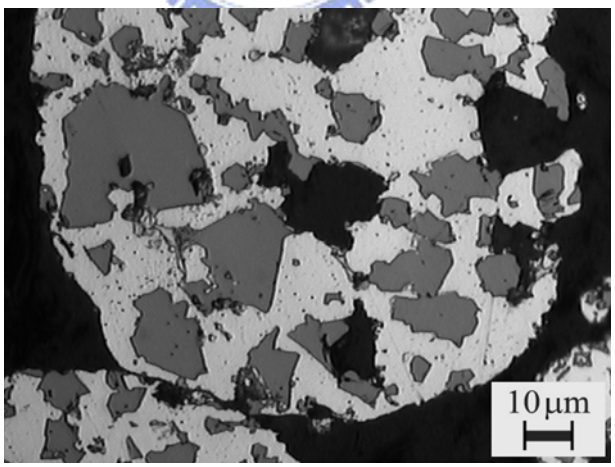

Figure 4.19 Optical microstructures of the as-atomized Al-25Si-2.5Cu-1Mg-0.5Mn powders after isothermally heat-treatment at (a) 500 °C, (b) 550 °C, and (c) 600 °C, for 1 hour.

The powders have particle size in range of 120~300μm.

B. Kinetics of Si grain growth

A series of isothermal heat-treatment tests were performed to clarify this Si grain coarsening behavior. Table 4.5 lists the results, which clearly show that the size of the Si grains increased with the heat-treatment temperature and period.

Table 4.5 Grain sizes of primary Si particle (μm)

Time (hr)	Isothermal Heat-Treatment Temperature (°C)						
	500	540	550	560	570	580	600
1	7.5 ±2.5	9.9± 4.8	10.8± 8.4	11.0 ±4.0	17.2±11.7	18.9 ±5.7	22.8±9.9
2	8.7 ±2.7	10.8 ±5.6	12.4 ±5.1	13.4 ±5.4	21.6±8.9	24.6 ±14.1	28.5 ±10.7
4	8.8 ±2.8	12.8± 7.9	13.3 ±6.5	15.9 ±7.2	27.7±11.4	31.5 ±18.1	35.5 ±11.9

** Those are measured from the coarse powders (120~300μm) and lists as a function of isothermal heat-treatment temperatures and time intervals*

** The Si particle size in the as-atomized powder is 8.1 ±2.7μm*

The kinetics of Si grain growth in the semi-solid state must be determined for thixocasting hypereutectic Al-Si alloys with fine Si grains.

. The driving force of Si grain growth is a decrease in the interfacial energy, due to a reduction in both the amount and the curvature of the Si grain-matrix interface. The classical Lifshittz Slyozov Wanger (LSW) theory [85-87] was applied here to analyze the grain growth behavior. For sparsely distributed spherical grains in a matrix under diffusion-controlled growth, the classical LSW theory predicts that the ripening process will yield a steady-state distribution of grain sizes and will cause the mean grain diameters (d) to increase with time (t) as [88-92]:

$$d^3 - d_0^3 = 32K\,t\,/9 \quad \text{.....(1)}$$

where d_0 is the initial mean grain diameter, K is a rate (kinetic) constant given as follows:

$$K=2DCV_m\gamma/(RT) \quad \text{.....(2)}$$

where D is the diffusivity of the grain element through the matrix, C is the concentration of the grain element in the matrix, V_m is the molar volume of the grain, γ is the grain-matrix surface energy, R is gas constant, and T is the absolute temperature. Figure 4.20 illustrates the Si grain size variations with isothermal heat-treatment time intervals and temperatures. The experimental values of Si grain sizes were plotted with discrete points and these points were line fitted using Equation (1). The grain growth behaviors are consistent with the calculation using Eqation (1). The grain-growth rate constants (K) at various isothermal heat-treatment temperatures can be determined from the gradients in Fig. 4.20. Since the diffusion involved in Si grain growth is thermally activated, the calculated rate constants (K) should depend exponentially on temperature; that is, they should be proportional to exp(-Q/RT), where Q is the activation energy. The value of Q can be obtained from the plot of the logarithm of the rate constant (K) against 1/T, as shown in Fig. 4.21. Figure 4.21 clearly shows that the rate constants in the semi-solid state fall into two distinct ranges. The rate constants at temperature below 565°C are around one order of magnitude lower than those at a temperature above 565°C. The calculated Q was 229 kJ/mol at a temperature below 565°C and 174 kJ/mol above 565°C. In this case, increasing the isothermal heat-treatment temperature also increased the liquid content in the matrix. Hence, the calculated activation energies slightly differ from the activation energy of diffusion of Si in an Al matrix at 500°C, 126-138 kJ/mol [93].

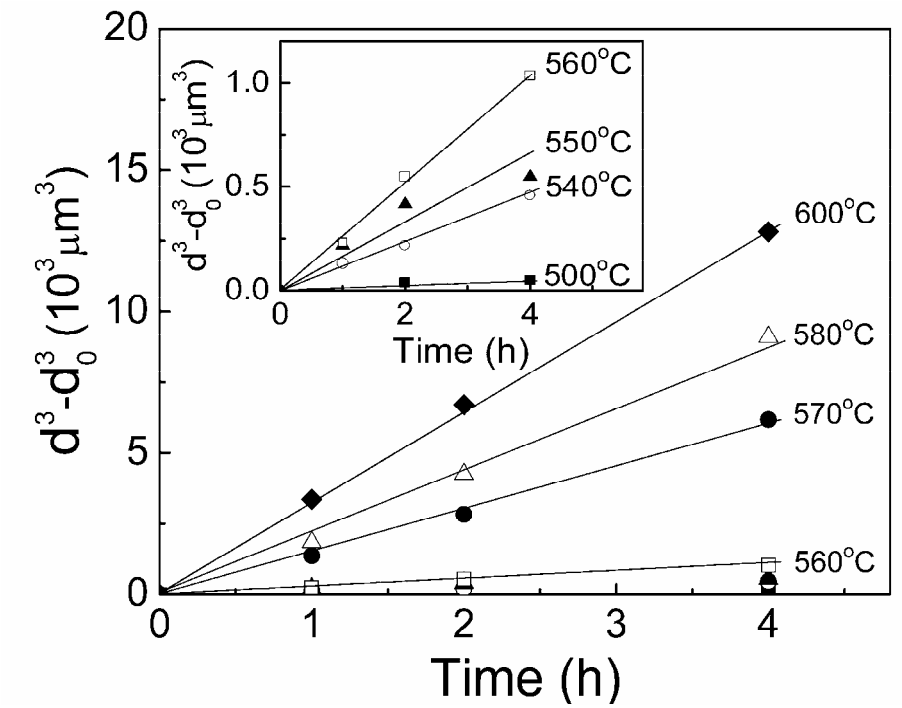

Figure 4.20 Evolution of the average Si grain sizes (d) as a function of isothermal-heat treatment temperatures and time intervals in the Al-25Si-2.5Cu-1Mg-0.5Mn powders

(in size of 120~300μm) d_0 is the average Si grain sizes in the as atomized powders. The experimental values of Si grain sizes were plotted with discrete points and these points were line fitted according to the LSW theory. The inset shows the magnified graph for the temperature ranged from 500℃ to 560℃.

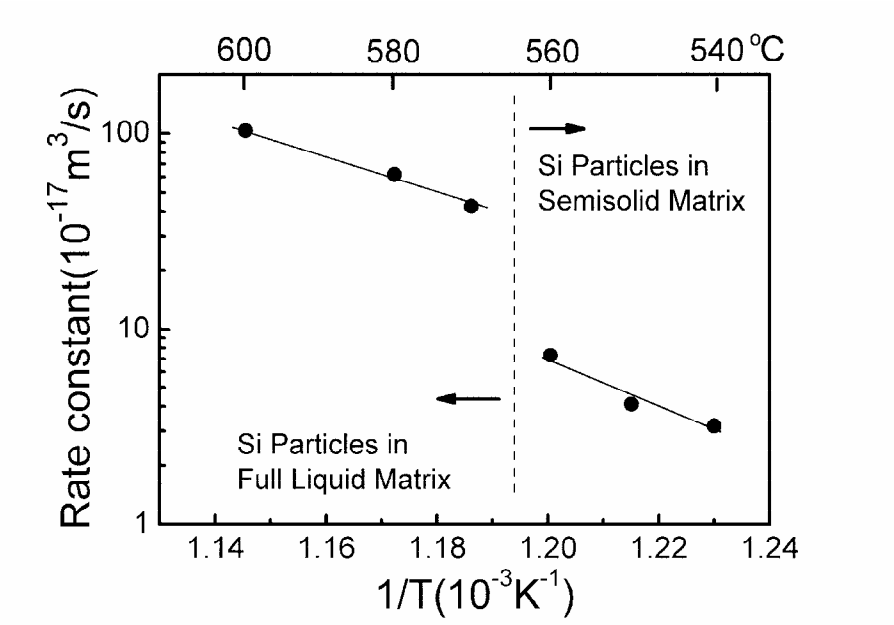

Figure 4.21 Si grain growth versus the inverse of isothermal heat-treatment temperatures.

Rate constants were obtained from linear dependence of the slope in plot Fig.4.20.

Figure 4.22 schematically depict that the matrix of Si grains is in the semi-solid state from 540°C to 565°C and in the liquid state above 565°C. Considering the thixocasting temperature used in this work, Si grain growth occurs by the transport of solute through the matrix. Equation (2) shows that K is proportional to both diffusivity (D) and solubility (C). For a binary Al-Si alloy, the Si solubility in the liquid melt at 577°C is 12.5 wt%, which is much higher then that in α-Al solid, 1.65 wt%. Furthermore, the Si diffusion coefficient in liquid Al melt is much higher than that in solid Al matrix. For example, the Si diffusion coefficient in the solid Al matrix at 497°C is only 1.6-2.2×10^{-9} cm^2s^{-1} [93], while that of Si grains in Al melt at 700°C is only 81×10^{-5} cm^2s^{-1} [94]. Accordingly, Si grain ripened more quickly in the liquid matrix than in the semi-solid matrix, since both the diffusivity (D) and the solubility (C) of the Si in liquid Al is much higher than in solid Al. The addition of Cu in hypereutectic Al-Si alloy effectively stabilized solid α-Al in semi-solid state. This addition of Cu is considered to be the critical part for the novel process presented herein, for fabricating a hypereutectic

Al-Si-Cu alloy with fine and evenly distributed primary Si grains.

As a summary the above experimental results, the Si particles coarsened slowly during isothermal heating at temperature below 565°C, but grew quickly above 565°C. This is because that if the powder at temperature below 565 °C contained the solid phases of α-Al grains and primary Si particles, as well as a small amount of liquid surrounding the solid phases. However, if it at temperature above 565°C, only the primary Si particles remained, suspended in a high volume of liquid phase. At former case, the presence of α-Al solid grains can prevent the Si particles from coming into direct contact with the liquid phase, since most of primary Si particles are imbedded in the solid α-Al. In addition, because the diffusion rate of Si in solid α-Al is much lower than that in a liquid melt, the Si particles grew slowly in this case. On the other hand, at the latter case the Si particles in the powder were suspended in the melt. This would cause rapid coarsening of the Si particles associated with the increasing Si diffusion rate in the melt.

Basing on the above discussion, it is suggested that the presence of solid α-Al grains in the semi-solid state can effectively prevent the primary Si particles from quick growth. This is the reason why a final semi-solid temperature of about 550°C, shown in Fig.4.7, was used for powder thixocasting in this study.

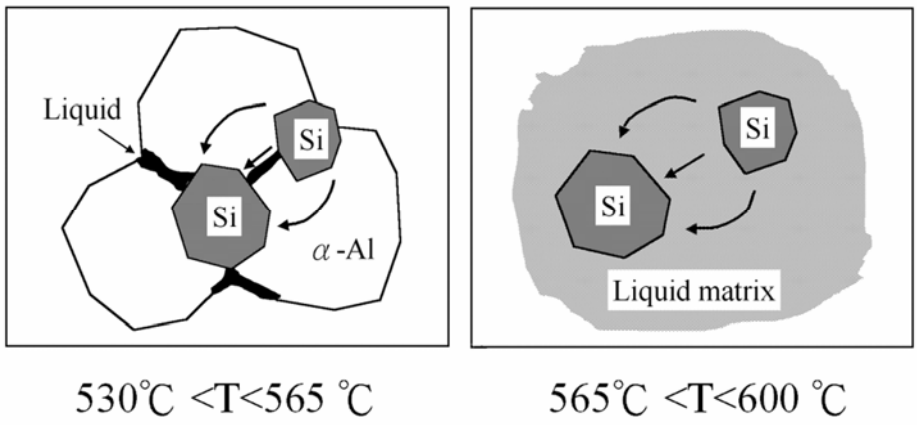

Figure 4.22 Schematic diagrams of diffusion paths for Si grain growth showing Si is transported through the Al alloy matrix, which is in semi-solid state at 530-565°C, and in liquid state at 565-600°C.

4.3.4 How to Eliminate Oxide Films and Pore Defects

How to effectively consolidate powder particles is also considered to be difficult in powder thixocasting process, because oxide films on powder surfaces and inter-granular pore in powder preforms must retard the consolidation. Three processing parameters were studied here to improve the consolidation strength of the powder-thixocast alloys.

1. Powder particle size: three kinds of powder size were used, fine (<45μm), medium (45~120μm) and coarse (120~300μm).

2. Density of powder preforms: two kinds of preforms were used, those were consolidated at 500 and 550°C with relative density of 74% and 90% respectively.

3. Extent of plastic deformation of preforms during thixocasting: three segments of thixocast samples, Biscuit, Runner, and Plate, as shown in Fig.4.13, were experienced different amount of plastic deformation.

Experimental results including tensile strength, densities, and microstructure are detailed and discussed as follows.

A. Density and tensile strength values of the powder-thixocast specimens

Tensile strength and density values of the powder-thixocast specimens were found to be depended on powder particle size, consolidating temperature and extent of plastic deformation during thixocasting.

Table 4.6 shows the density values of the powder-thixocast specimens fabricated using powder preforms consolidated at 500°C and 550°C. The powder preforms have much higher relatively density after they were thixocast, as is noted by comparing Table 4.3 with Table 4.6, indicating that most of the inter-granular pores in the powder compacts were eliminated by thixocasting. Table 4.6 also shows that the relative density of the thixocast samples did not seem to be affected by the factors of preform consolidating temperatures and specimen positions. However, these two factors greatly influence the consolidation strength of the powder-thixocast specimens (Table 4.7), which will be discussed in the followings.

Table 4.7 shows that the thixocast specimens fabricated with compacts consolidated at 550°C are stronger than those with compacts consolidated at 500°C. Inter-granular pores and oxides were considered to explain this difference. Since the difference between the relative densities of these two thixocast specimens is small (Table 4.6), the strength difference is associated primarily with the interfacial oxides. Figure 4.15 (a) shows that the powder compacts consolidated at 500°C have many inter-granular pores, resulting in poor bonding between individual powder particles. This weak bonding cause that the deformation of the powder compacts takes place by rotating or sliding of individual powder particles during thixocasting. This rotation or sliding does not easily rupture the surface oxides on the powders.

Table 4.7 lists the ultimate tensile strengths of the powder-thixocast specimens measured from different sections of the thixocast specimens, as depicted in Fig.1(e). Notably, the tensile strengths varied greatly from section to section of the powder-thixocast specimens. The specimens were strongest in the “plate” section and weakest in the “biscuit” section. For example, for the thixocast specimens fabricated from powders of fine size (<45μm) and compacts consolidated at 550℃, the strength of the “runner” (129.7MPa) and the “plate” (210.3MPa) were increased by 62% and 120%, respectively, over that of the “biscuit” (95.7MPa). Table 6 also shows that the powder-thixocast specimens fabricated from smaller powders exhibited a slightly lower tensile strength. The thixocast specimens fabricated using the powder compacts consolidated at 550℃ clearly had a higher tensile strength than those fabricated using compacts consolidated at 500℃.

The strength values of the powder thixocast are close to those obtained by P. J. Ward [35,36], who thixocast the hypereutectic Al-Si alloys using feedstock made by spray forming followed by extrusion. This may indicate that powder preforms could be effectively consolidated by powder thixocasting. This hypothesis also can be verified from Table 4.7, showing that the thixocast specimens with smaller powders exhibit somewhat worse mechanical characteristics, owing to the larger specific oxide surface areas of the smaller powders. This result may further support the above hypothesis that surface oxide films play a vital role on the strength degradation of powder-thixocast

specimens. Because the smaller powder size results in the larger amount of oxide films in the powder preforms, which leading to lower consolidating strength if the oxide films were not broken down.

Figure 4.23 shows that a typical tensile fractograph of a powder-thixocast sample that used preforms consolidated at 500°C exhibit many dimples and cleavage planes. However, besides these dimples and cleavages, several deep spherical caves also can be noted, which may be the evidence of the de-bonding of individual powder particles. In other words, these spherical caves were considered to be formed by the decohesion of the powder particles from their oxide interfaces, resulting from incomplete elimination of the detrimental oxide film on the powders after thixocasting. However, the deep spherical caves was not found in the thixocast specimens fabricated using powder compacts consolidated at 550°C. The result further supports our aforementioned assumption that the powder compacts consolidated at 500°C still have large amount of inter-granular pores (relative density of 74%), so that each individual powder particles may be less deformed to rupture the oxides during the thixocasting, decreasing their consolidated strength.

Table 4.6 Densities of powder-thixocast Al-25Si-2.5Cu-1Mg specimens.
The specimens were measured in different positions depicted in Fig. 4.13 and were thixocast using the powder preforms consolidated at different temperatures

	Consolidating Temperatures					
	500°C			550°C		
Specimen position	Biscuit	Runner	Plate	Biscuit	Runner	Plate
Density	2.558	2.556	2.606	2.596	2.569	2.609
Relative density (%)	96.5	96.4	98.2	97.9	96.8	98.4

Table 4.7 Ultimate tensile strengths (MPa) of the Al-25Si-2.5Cu-1Mg-0.5Mn thixocast specimens in different positions depicted in Fig. 1(e) and using the powder compacts consolidated at different temperatures

Powder size	Consolidating Temperatures					
	500°C			550°C		
	Biscuit	Runner	Plate	Biscuit	Runner	Plate
<45μm	*	89.6 ±11.9	178.0 ±10.7	95.7 ±59.2	129.7 ±32.0	210.3 ±13.4
45~120μm	*	128.6 ±17.8	163.4 ±28.0	152.1 ±53.6	184.4 ±20.4	210.7 ±5.0
120~300μm	_	_	193.2 ±25.2	_	_	224.7 ±4.5 (304±6.5)

* Materials are so brittle that tensile specimen can't be machined.

± Standard deviation

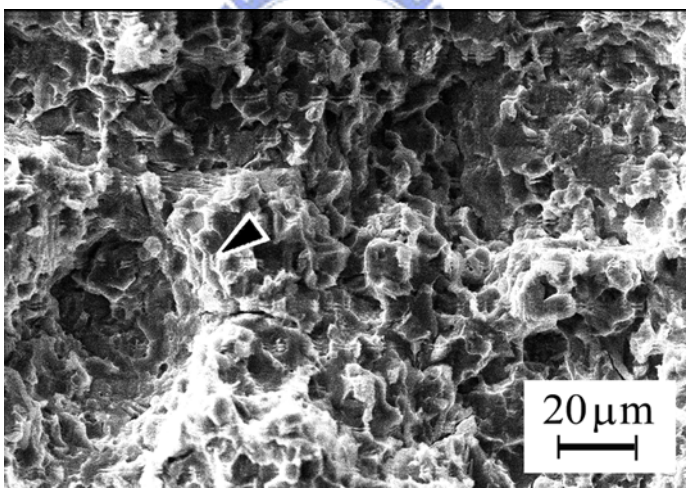

Figure 4.23 Pull-out of powder particles observed on a tensile fractograph of a powder-thixocast specimen.

The specimen was fabricated using powders in size of 45~120μm and compacts consolidated at 500℃. ▽ indicates spherical caves caused by powder decohesion.

B. Microstructures of powder-thixocast specimens

The above experimental results show that the powder samples were more strongly consolidated when they were fabricated using larger-sized powder and higher plastic deformation. These results are attributed to the oxide films on powder surface. The following microstructure results will show the direct evidence of this hypothesis of powder consolidating strength associated with oxide films.

Figure 4.24 is the typical microstructure of a powder-thixocast specimen, showing fine and evenly distributed Si grains. It shows that both oxide layers on the powder interfaces and the inter-granular pores (Fig.4.15) almost vanished after thixocasting, implying that the new powder-thixocasting process presented herein can effectively consolidate the Al-Si powders.

Figure 4.25 displays the optical micrographs of the powder thixocast sample observed from the longitudinal section of the "Runner" segment. In traditional powder extrusion hypereutectic Al-Si alloys, there are apparent texture microstructures or flow lines alloy the extrusion direction [95]. In Fig. 4.25, however, there was no sign of clustering of alignment of certain phases, possibly following the flow lines, indicating that the deformation of individual powder particles could not be the primary mechanism for the preform deformation.

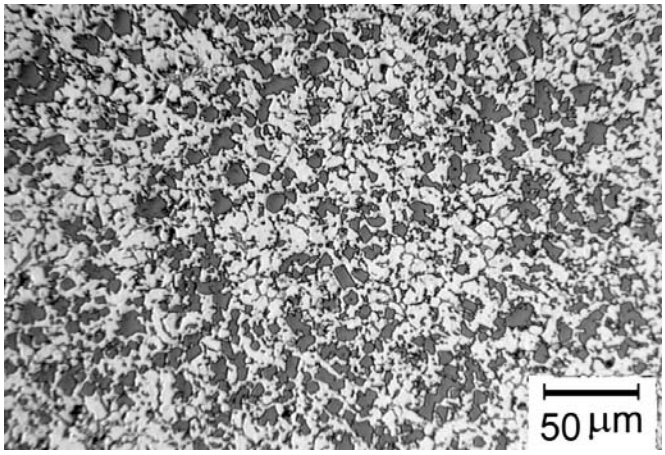

Figure 4.24 Optical micrographs of the powder thixocast sample observed from "Plate" segment.

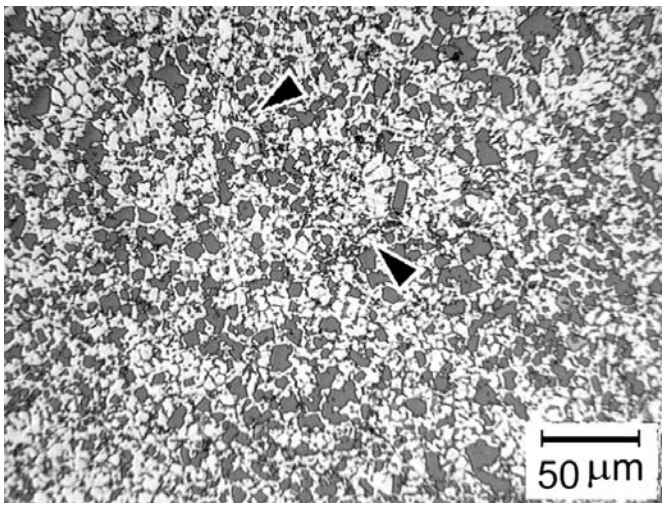

(a)

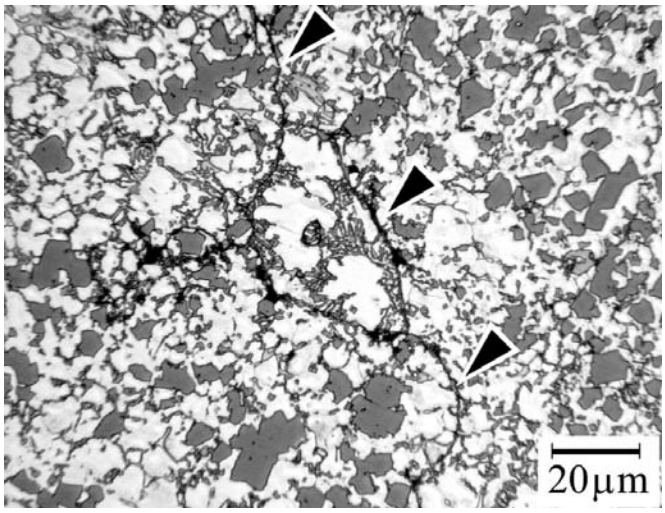

(b)

Figure 4.25 Optical micrographs of the powder thixocast sample observed from (a) "Runner" segment in the longitudinal section. (b) Enlarged micrographs observed from the same sample. Arrows indicate the oxide films.

C. Consolidating mechanisms in powder thixocasting

In an attempt to understand the consolidation mechanism in powder thixocasting, tensile properties of the as-thixocast specimen at the three segments indicated in Fig.4.11 were examined. The three segments may correspond to the three levels of deformation on the powder preform. During powder-thixocasting, the semi-solid compact materials were first forged from a diameter of 76 mm to a diameter of 84 mm to fill the mold "biscuit" cavity. The materials were then extruded into the “runner” cavity in a process like forward extrusion with a ratio of 7.84 and a 90° angular extrusion. Finally, the materials were extruded to "plate" cavity from a thickness of 20 mm to 6 mm. Therefore, the specimens machined from “plate” section clearly experienced the largest extent of deformation, and those from “biscuit” section experienced the smallest extent of deformation.

In Table 4.7, maximum UTS values of these three segments of “biscuit”, “runner”, and “plate” were 125, 175, and 224 MPa, respectively. The strength of the “runner” and the “plate” were increased by 28 % and 79 %, respectively, over that of the “biscuit”. This strength improvement corresponds to the deformation levels in these segments. That is, the more deformation of the powder preforms after thixocasting, the higher the strength of the consolidated powder that would be obtained. Therefore, we suggest that the mechanism of powder consolidation in powder thixocasting may resemble that in powder forging or extrusion.

The maximum tensile strength of the specimens in Table 4.7 is 225 MPa, and that of the T6 specimen is 304 MPa. The strengths are comparable with those obtained by P. J. Ward [35,36], who uses extruded spray-forming billets to thixocast the hypereutectic Al-Si alloy. Since the extruded spray-forming billets exhibit few oxide films and pores, this comparable values of strength may indicate the detrimental oxide films and pores of the powder performs are approximately eliminated after powder thixocasting.

The above discussions suggest that the mechanism for consolidating powder by plastic deformation is also adequate for powder thixocasting process here. However, the behaviors of individual powder particles in preforms during powder thixocasting and conventional powder forging could differ significantly. In powder forging, preform

deformation generally is accompanied by plastic deformation of individual powder particles, producing strain-hardening as well as the creation of microstructures of dislocation tangles, textures or flow lines [95,96]. However, these microstructure features were not observed in the powder thixocast samples, as is discussed in Section 4.3.4 B above.

Figure 4.26 schematically illustrates the movement of individual powder particles during thixocasting in a semi-solid state. We postulated that the preform deformation was mostly modulated by the rotation and sliding of the individual powder particles and the individual solid α-Al grains or Si particles, rather than by the deformation of individual powder particles. Because of this postulated deformation model, the thixocast sample seldom displayed flow lines. Furthermore, the oxide films on the powder particle surface could be difficultly broken down into small pieces by powder thixocasting without severe preform deformation. This expectation is correct, since continuous oxide films were noted to occasionally appear in the “runner” segment (Fig.4.25), yet oxide films almost failed to appear in the “plate” segment (Fig. 4.24). Since the “biscuit” and “runner” may only act as an ingate in the thixocast sample, the existence of the oxide films in these volumes is considered not to influence the application of the powder thixocasting.

Figure 4.26 shows the expected behavior of a powder preform during deformation under a semi-solid state. Owing to this mechanism, the preform can easily be deformed into complex shapes. In conventional PM, however, the powder preforms do not have such a good deformability, therefore, additives such as binders or lubricant must be premixed with metal powders to improve the flowability of powders and to achieve an adequate formability [97, 98]. However, these additives usually degrade the properties of the sintered alloy. Powder thixocasting take the advantage of no such a problem, since no such additives are needed.

From Fig. 4.26, it may be understood that the oxide film on the powder surface may be break down into small pieces by mutual slide between each powder particles, whereas, the rotation of individual powder particles has less effect on eliminating the oxide film. Rotation of individual powder particle is more easily in a lose powder

preform, which may explain why the powder-thixocast using powder preforms consolidated at 500 ^{o}C has less mechanical strength than that at 550 ^{o}C.

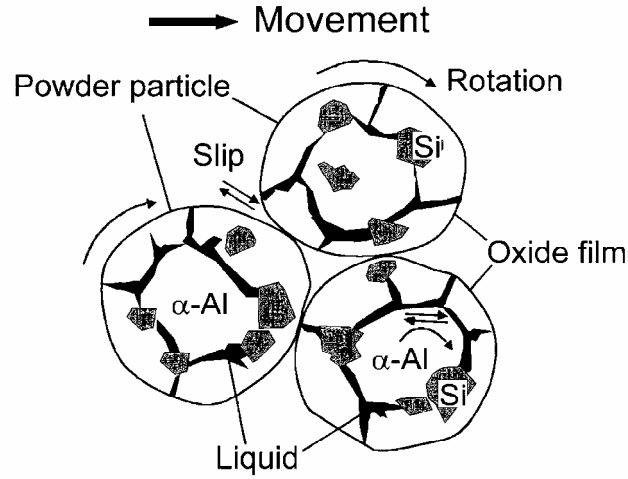

Figure 4.26 Plastic deformation at semisolid state of a powder preform

4.4 Demo Part Fabrication

This section presents the experiments for fabrication a demo part, a compressor scroll, to further demonstrate the feasibility for net-shape forming of Al-25Si-2.5Cu-1Mg alloy by powder thixocasting. Based on the above experiments, it was known that the following procedures should be obeyed:

1. Microstructural coarsening during thixocasting is avoided by maintaining the processing temperature between 540 °C and 560°C, so that the primary Si particles can growth slowly in Al-25Si-2.5Cu-1Mg alloy.

2. The short heating time by induction coil can minimize the oxidation, even though the powder was heated in air.

3. The oxide films and the inter-granular pores in the powder compacts should be effectively eliminated by a large plastic deformation during powder thixocasting.

Gating system design in powder-thixocasting mould

Because of the third item mentioned above, the mould design in gating system, including the shape, size and positions of the gates and runner, was considered important for obtaining a highly-consolidated thixocast product. This is because an adequate design of gating system can deform the preform severely.

In traditional PM, it is known that the mechanical strength of a PM specimens can be effectively improved by increasing plastic deformation of the powder preforms, since the deformation close the inter-granular pores and disrupt the oxides to facilitate welding of the powder particles [10-17]. In order to obtain large shear deformation, a method called " double shear extrusion process" was introduced by Hoshino [99]. Figure 4.27 schematically shows this process. It was found that the consolidated powders by this process have better ductility than that by conventional extrusion. The plastic deformation mechanism in double shear extrusion can be simply explained using the equal-channel-angular extrusion (ECAE) process [100,101], as is shown in Fig 4.28. When a metal passes the ECAE channel, a pure shear deformation occurs at the plane A-A (Fig.4.28 a). After each pass, the metal has an increment of strain

intensity: $\Delta\varepsilon = \frac{2}{\sqrt{3}}\cot\phi$ [100].

The shear strain by ECAE is very large. For instance, if a metal once go through the channel of an ECAE of φ=45°, it is deformed like that it is extracted by a tensile test to an equivalent elongation of 220% [101].

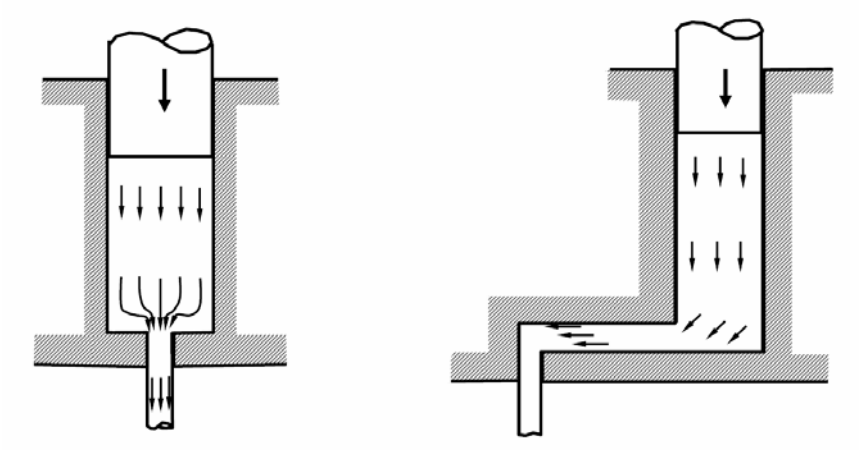

(a) (b)

Figure 4.27 Extrusion methods, (a) conventional extrusion, (b) double shear extrusion [99]

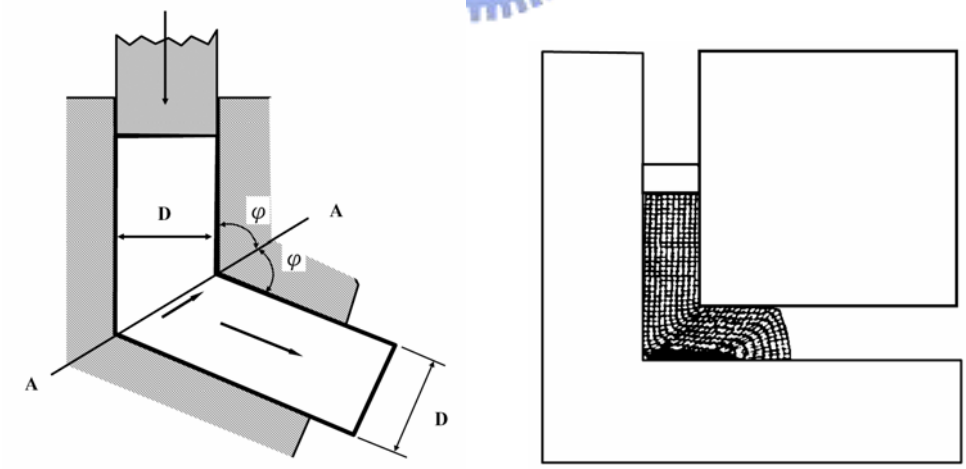

(a) (b)

Figure 4.28 (a) Equal channel angular extrusion, (b) simulation by finite element, φ=45 [100]

According to this concept, a die-mold with center gate and long runner shown in Fig. 4.11 was designed to obtain large shear deformation of the powder perform upon thixocasting. Since the powder perform is injected through gating system, i.e. sprue/or gate and runner, to the die cavity of product, a suitable designed gating system can make large plastic deformation of powder preform during thixocasting.

Formability and microstructures of the demo part

Figure 4.27 shows a product made of hypereutectic Al-25Si-2.5Cu-1Mg powder using the procedure described above. This product shows good appearance, indicating good formability and feasibility of net-shape forming in this powder thixocasting process.

Figure 4.27 a shows schematic diagram of the die used to thixocast a compressor scroll. A side gate and long sprue were designed to obtain large deformation of the powder performs during thixocasting. Figure 4.27 b demonstrates the scroll produced by the novel thixocasting method, showing good formability and no apparent defects. Figure 4.27 c shows the microstructures of the scroll, indicating uniform distribution of primary Si particles with size about 15~25m.

(a)

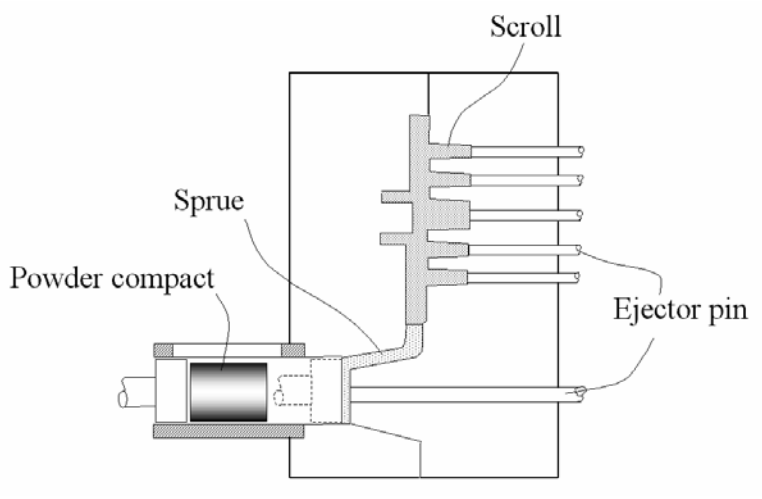

(b)

(c)

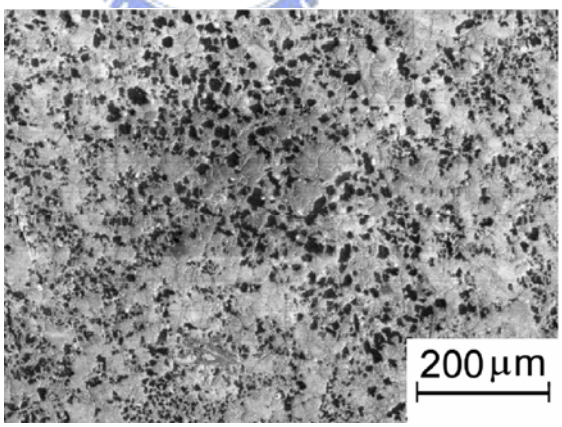

Figure 4.27 A powder-thixocast compressor Al-25Si-2.5Cu-1Mg scroll

The component is made of gas-atomized powder and thixocast in conventional high-pressure die casting equipment. (a) Schematic drawing of the die-mold, (b) the thixocast product and (c) SEM microstructure of the product.

4.5 Conclusions

This Chapter presents a novel method, which combines consolidating prealloyed powders with thixocasting the consolidated compacts, for net-shape forming of a hypereutectic Al-25%Si-2.5%Cu-1Mg-0.5Mn alloy.

Following conclusions can be drawn about the success of this process.

1. The powder preforms exhibit very good formability by this unique process. The powder thixocast products have satisfied strength and substantial structure with uniform distribution of fine Si particles, while the processing temperature is suitably controlled.
2. The Al-Si-Cu-Mg powder preforms used for thixocasting should be dense enough to have sufficient strength and low porosity for handling and heating with an induction coil. To obtain powder preforms of high density and at a relatively low pressure, the Al-Si powder could be hot pressed while in a semi-solid state.
3. By elemental addition of 2.5 wt% Cu into the hypereutectic Al-Si alloy, α-Al grains could be stabilized to coexist with Si grains and melt in the powders. About 18 wt% melt was formed in the powder compacts when the compacts were heated to 560°C. The melt wet the solid α-Al and Si grains, thus the compacts could be deformed easily during thixocasting in semi-solid state. However, the stabilized α-Al grains would melt completely when the powder compacts were heated above about 565 °C. Thus the Si grains became suspended in the melt, and that leading to extreme Si grains growth.
4. Two distinct ranges of Si grain growth were found in semi-solid state of the powders. According to the LSW theory, the activation energies of Si grain growth were calculated to be 174 kJ/mol at temperatures above 565°C and 229 kJ/mol below 565°C. The rate constants of Si grain growth at temperatures above 565°C are around one order of magnitude than those at temperatures below 565°C. Therefore, heating the powder compacts to the temperature between 540°C and 560°C ensured adequate fluidity of the compacts and prevented the Si grains from coarsening rapidly during thixocasting.

5 In powder thixocasting, inter-granular pores of powder preforms can be effectively eliminated just after thixocasting, however the strength of thixocast samples needs to be effectively improved by using high density of powder preforms and increasing plastic deformation of the preforms. A consolidation mechanism is proposed to explain these results. Powder particles rotating and sliding are the main mechanism that responsible for deformation strain of preform during thixocasting. More plastic deformation during thixocasting increase the opportunity to breaking down powder oxide films, larger-sized powder and quick heating of the preforms decrease the amount of surface oxide films. All these adequate methods may result in high strength of powder-thixocast alloys.